DETECTION OF VERY WEAK TRANSMISSIONS FROM DEEP SPACE

Gary Noreen, Jet Propulsion Laboratory, 4800 Oak Grove Drive, Pasadena, CA

Peter Kinman, Case Western Reserve University, EEAP Dept., Glennan Bldg., Cleveland, OH

Robert Bokulic, Applied Physics Laboratory, Johns Hopkins University, Laurel, MD

ABSTRACT

Designers of future planetary missions often reduce spacecraft transmitter power and oscillator stability requirements to decrease mission cost. Unfortunately, these reductions can make it impossible to detect weak signals from deep space using conventional demodulation techniques.

The new Block V receiver being installed in the Deep Space Network (DSN) can recover suppressed carrier signals and can utilize very narrow loop bandwidths – as narrow as 0.1 Hz. However, operations at very narrow tracking loop bandwidths are quite sensitive to spacecraft oscillator stability. Low-cost oscillators planned for future missions can force the use of wide tracking loop bandwidths, leading to reduced carrier tracking performance. This reduced carrier tracking performance can, in turn, lead to a significant increase in required spacecraft transmitter power.

This paper presents the theory behind coherent detection of very weak telemetry from deep space. It then briefly recounts tests characterizing Block V performance for the NEAR spacecraft in two-way coherent operations and presents recommendations for mission designers.

INTRODUCTION

From the time of the very first deep space missions, telecommunications design efforts have focused on a continuing quest for ever higher data rates from ever higher ranges. The capabilities of the Deep Space Network (DSN) and of new spacecraft have been constantly growing, leading to an overall increase in high rate telemetry capability of twelve orders of magnitude from the early Pioneers to the upcoming Cassini spacecraft.

More recently, a new trend is emerging. In this era of “better, faster, cheaper” missions, designers are finding that they can tolerate lower data rates while still returning adequate science data to justify their missions.

The Galileo project is demonstrating that important science objectives can be achieved even with a very low data rate by being very selective about which data to return and by using data compression. Galileo has a 4.8 m unfurlable High Gain Antenna (HGA) that did not open properly after launch, rendering it useless. Galileo has had to make do with its S-band Low Gain Antenna (LGA) for all telemetry, reducing the planned data rate by five orders of magnitude. Yet this mission is still expected to meet 70% of its mission objectives.

Deep space telemetry has, from the start of the space program, been received using coherent tracking techniques. These techniques require the receiver to coherently re-

cover the downlink carrier from the received signal. The recovery process uses a narrow carrier tracking loop in order to ensure an adequate carrier signal-to-noise ratio.

New missions are doing everything they can to decrease costs. They generally plan to accomplish this, in part, by reducing spacecraft size. Decreasing spacecraft size generally results in lower transmitter power and lower antenna size. To make matters worse, few new missions are considering the use of Ultra-Stable Oscillators (USOs), which make it easier to receive weak signals with narrow tracking loop bandwidths. Their driving telemetry performance requirements frequently come not from meeting the maximum data rate through a high gain antenna, but from the need to be able to receive any data at all from a low power transmitter and a low gain antenna over a wide range of spacecraft attitudes at maximum range from earth.

Table 1 shows the maximum range at which each of a number of deep space missions are required to send telemetry to Earth through their low gain antennas. It calculates the EIRP of each and the Power Flux Density (PFD) received from each spacecraft at the surface of the earth. All numbers are at X-band except Galileo. Note that PFD at maximum range has relatively little variation between most of the non-Mars missions.

Mission	Xmit Pwr, W	LGA Gain, dB	Xmit Losses, dB	EIRP, dBW	Max Range, AU	PFD, dBW/m2	Oscillator
Galileo S-Band	20	6	-2	17.0	6	-233.0	USO
NEAR	5	6	-3	10.0	3.2	-234.6	Cassini Aux Osc
Mars Pathfinder	12.9	5.9	-1.1	15.8	1.5	-222.1	Cassini Aux Osc
Mars '96 Orbiter	26.5	6.9	-2.15	19.0	2.4	-223.1	MO Aux Osc
Cassini	19	9.2	-1.5	20.5	10	-234.0	USO
NM DS1	13	3	-2.5	11.6	2.5	-230.8	SDST Aux Osc
Mars '98 Orbiter	15	12	-2.5	21.3	2.67	-221.8	Cassini Aux Osc
Mars '98 Lander	15	12	-2.5	21.3	1.9	-218.8	Cassini Aux Osc
Solar Probe	5	7.5	-2	12.5	6	-237.6	SDST Aux Osc
Pluto Express	5	3	-2	8.0	2	-232.5	SDST Aux Osc

Table 1: Transmit Performance through LGAs

DEEP SPACE NETWORK

The Deep Space Network[1] consists principally of three complexes of large antennas near Canberra, Australia; Madrid, Spain; and in the Mojave desert of California. These antennas were designed and built to communicate with spacecraft in deep space. Each DSN complex has one 70 m antenna and two or more 34 m antennas. X-band receive performance of these antennas is summarized in Table 2 for 25° elevation angle. Gain G includes circuit and pointing losses; temperature T includes weather effects (90% weather). Table 2 shows per-

formance for both the existing maser Low Noise Amplifiers (LNAs) at the 70 m antennas and for proposed new HEMT LNAs.

Antenna	*70 m Maser*	*70 m HEMT*	*34 m BWG*
Gain, dBi	73.7	73.7	68.0
T, K Non-Diplexed	34	27.5	31.5
T, K Diplexed	42	27.5	42
G/T, dB/K Non-Diplexed	58.4	59.3	53
G/T, dB/K Diplexed	57.5	59.3	51.8

Table 2: DSN Antenna Performance

DSN antennas at Goldstone can be arrayed for brief periods of time under exceptional circumstances. In the case of perfectly efficient combining, the combined G/T (in units of reciprocal Kelvins) is equal to the sum of G/T (in units of reciprocal Kelvins) from the individual antennas. Typically, there is an inefficiency factor of about -0.2 dB associated with the combining.

BLOCK V RECEIVER

The new digital receiver of the DSN, the Block-V Receiver, offers a great deal more flexibility than the analog receivers which it replaces.[2] Most important, this new receiver offers the prospect of using very small carrier synchronization loop bandwidths. This has been made possible by the closing of the phase-locked loop after digitization within an intermediate-frequency stage. Thus, the loop is entirely digital, its parameters are numeric, and loop stability is much less of a problem.

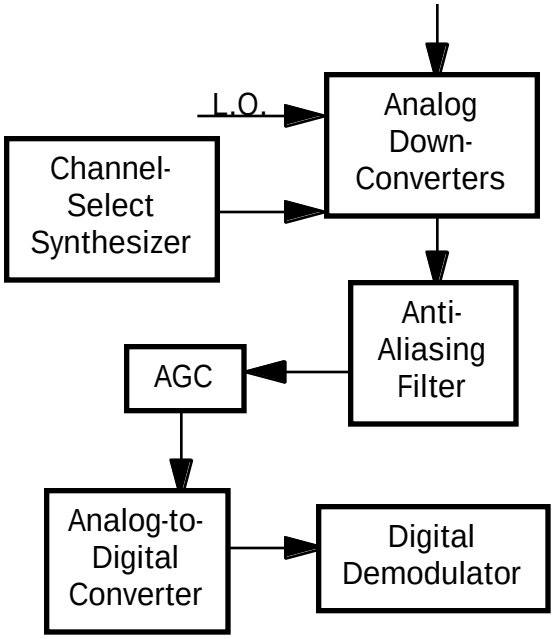

Figure 1: Block V Receiver

Figure 1 is a diagram of the Block-V Receiver. At the front of the receiver are multiple stages of analog downconversion. The hardware used within these stages depends on the band in which the downlink is operating. The Local Oscillators (L.O.) remain at a constant setting for the duration of a tracking pass. The channel-select synthesizer is adjusted before the beginning of a pass to a value appropriate for the channel (within the band) of the incoming downlink signal. The anti-aliasing filter is a necessary precursor to sampling, and the Automatic Gain Control (AGC) is a necessary precursor to quantization. Carrier, subcarrier and symbol synchronization are all performed digitally within the digital demodulator. The output of the receiver is a stream of soft-quantized symbols, suitable for input to a Viterbi decoder. Binary Phase-Shift Keyed (BPSK) telemetry of both the residual carrier and suppressed carrier type are supported.

SYSTEM ANALYSIS

The minimum Power Flux Density (PFD) that is required at the receiver in order to support telemetry of a given bit rate is estimated in this section. For the aperture antennas of the DSN, the PFD at the antenna is related to the total received signal power to noise spectral density ratio P_T/N_0 by

$$\frac{P_T}{N_0} = \frac{(\text{PFD})A\eta_A}{kT} \qquad (1)$$

where A is the projected area of the antenna onto a plane that is perpendicular to the antenna boresight, η_A is the antenna efficiency, T is the receiving system noise temperature referenced to the antenna feed, and k is the Boltzmann constant, 1.380622×10^{-23} W/(Hz•K). In decibel units, the Boltzmann constant is -228.6 dBW/(Hz•K). Equation (1) assumes that the antenna is correctly pointed and that the incoming signal is circularly polarized to match the antenna. The DSN antennas are ordinarily characterized by antenna gain G, rather than by A and η_A; these quantities are related by

$$G = \frac{4\pi f^2 A\eta_A}{c^2} \qquad (2)$$

where f is frequency and c is the speed of light in vacuum. The substitution of equation (2) in equation (1) yields the more convenient expression

$$\frac{P_T}{N_0} = \frac{c^2(G/T)(\text{PFD})}{4\pi f^2 k} \qquad (3)$$

The minimum P_T/N_0 that is required to support a given bit rate depends, of course, on the modulation and coding schemes that are used. This minimum P_T/N_0 is independent, however, of the properties of the antenna. Thus, at this point in the analysis it is convenient to focus attention on P_T/N_0.

Later, the antenna G/T is taken into account through equation (3) in determining the minimum required power flux density.

In this report, consideration will be given to two different (but related) modulation schemes: residual-carrier BPSK and suppressed-carrier BPSK. With both schemes, each binary symbol to be conveyed is impressed upon the carrier by a shift in phase of either plus or minus θ radians, depending on whether the symbol is a logical one or logical zero. If this θ, the modulation index, lies within the range $0° < \theta < 90°$, a residual carrier is present. The residual carrier is the specular power at the carrier frequency that is used by the receiver for carrier synchronization.[3] The power in this residual carrier is $P_T \cos^2\theta$, where P_T is the total signal power. The remainder of the signal power, $P_T \sin^2\theta$, lies in the modulation sidebands. A judicious choice of the modulation index is an important part of telemetry link design, as it determines the allocation of power to the residual carrier and the modulation sidebands. If $\theta = 90°$, no residual carrier is present: the carrier is suppressed. The motivation for suppressing the carrier is that this allocates all of the signal power to the message-carrying sidebands, eliminating the inefficiency associated with diverting some of the signal power to a specular residual carrier. With suppressed-carrier telemetry, carrier synchronization can be achieved with a receiver that employs a Costas loop, a kind of phase-locked loop that extracts the carrier frequency and phase from the modulation sidebands. [3] For all but the smallest telemetry bit rates, suppressed-carrier telemetry is more efficient than residual-carrier telemetry. For very small bit rates, however, it

turns out that a residual carrier with an optimized modulation index is preferred.

Only one coding scheme is considered in this report: a concatenation of a Reed-Solomon (255, 233) code with a convolutional (k=15, r=1/6) code. This coding scheme is typical of the kind used for deep space telemetry.

Telemetry will be successfully demodulated and decoded if and only if two constraints are simultaneously met. There must be an adequate energy per bit to noise spectral density ratio E_b/N_0 for the demodulated baseband symbols as delivered to the decoders, and there must be an adequate signal-to-noise ratio in the carrier phase-locked loop. The second constraint is necessary since coherent demodulation is used, which requires carrier synchronization. For the concatenated coding scheme considered here, the first constraint will be met if

$$\frac{E_b}{N_0} = \frac{P_T}{N_0} \cdot \frac{\eta_{SL} \sin^2 \theta}{R_b} \geq 0.3 \text{ dB} \qquad (4)$$

where R_b is the information bit rate and η_{SL} is an efficiency factor called "System Loss," generally comprised of radio loss η_{RL} and various lesser distortion and synchronization losses. When this constraint is met, a Bit Error Rate (BER) of 10^{-5} or better will be achieved. An η_{RL} that is less than 1 arises when the carrier synchronization is imperfect.

Figure 2 plots η_{RL} as a function of phase error variance σ_ϕ^2 in the carrier phase-locked loop for the case of residual carrier with a 2 Hz loop bandwidth and R_b = 10 bps. (The η_{RL} curve for other values of loop bandwidth and R_b are numerically close to this curve and so are not shown here.) The second constraint that must be met if telemetry is to be successful is

$$\sigma_\phi^2 \leq \begin{cases} 0.10 \text{ rad}^2, & \text{Residual Carrier} \\ 0.02 \text{ rad}^2, & \text{Suppressed Carrier} \end{cases} \qquad (5)$$

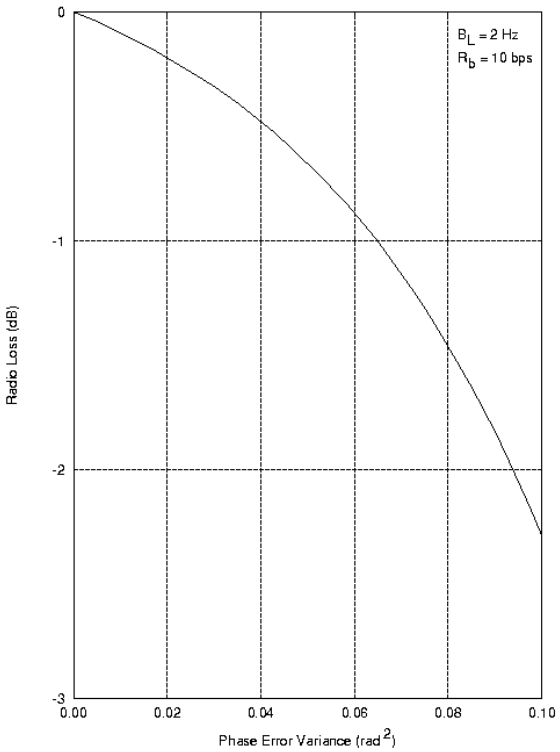

Figure 2: Radio Loss

σ_ϕ^2 must be smaller for suppressed carrier than for residual carrier because the loop that tracks suppressed carrier, the Costas loop, is susceptible to half-cycle slips.[4] The result of a half-cycle slip is an inversion of the demodulated symbol stream. The phase error variance of the carrier phase-locked loop generally has two components.

$$\sigma_\phi^2 = \frac{1}{\rho_C} + \sigma_o^2 \qquad (6)$$

The first component is the result of thermal noise; ρ_C is the signal-to-noise ratio in the carrier phase-locked loop. The second component is the result of phase noise on the

arriving carrier; σ_o^2 is the contribution of this phase noise to the phase error variance.

The signal-to-noise ratio in the carrier phase-locked loop is given by

$$\rho_C = \begin{cases} \frac{P_T}{N_0} \cdot \frac{\cos^2\theta}{B_L}, & \text{Residual Carrier} \\ \frac{P_T}{N_0} \cdot \frac{\eta_{SQ}}{B_L}, & \text{Suppressed Carrier} \end{cases} \quad (7)$$

where B_L is the bandwidth of the loop and η_{SQ} is the "Squaring Loss" of a Costas loop, which is given by

$$\eta_{SQ} = \frac{2(E_S/N_0)}{1+2(E_S/N_0)} \quad (8)$$

The energy per symbol to noise spectral density ratio E_S/N_0 is defined by

$$\frac{E_S}{N_0} = \frac{P_T}{N_0} \cdot \frac{r}{R_b} \quad (9)$$

where r is the code rate.

The contribution of phase noise to phase error variance depends on the quality of the oscillator. For one-way transmission, the one-sided power spectral density of the phase noise $S_o(\cdot)$ typically varies as

$$S_o(f) = \frac{S_o(1)}{f^3} \quad (10)$$

in the vicinity of 1 hertz, where f is the Fourier frequency. $S_o(1)$ is related to the measured number of dBc/Hz at 1 Hz offset from carrier, denoted here $L_o(1)$.[5]

$$S_o(1) = 2 \cdot 10^{L_o(1)/10} \quad (11)$$

The σ_o^2 that results from phase noise with $S_o(f)$ of the form given in equation (10) is, for a second-order standard underdamped phase-locked loop,

$$\sigma_o^2 = \frac{8.7 S_o(1)}{B_L^2} \quad (12)$$

For oscillators with a lot of phase noise, it is necessary to increase the B_L of the receiver in order to keep σ_o^2 at an acceptable level. For the three oscillators under consideration in this report, the key parameters are listed in Table 3. Included within this table is the recommended B_L and the resulting σ_o^2. For two-way transmission, the downlink phase noise is dominated by thermal noise that originates in the spacecraft transponder. In this case, σ_o^2 is approximately

$$\sigma_o^2 = \frac{C_T^2}{\rho_T} \quad (13)$$

where the transponder frequency turnaround ratio $C_T = 880/749$ for X-band up and down. ρ_T is the signal-to-noise ratio in the transponder phase-locked loop. Its value varies widely from one mission scenario to another. In this report a conservative value of 15 dB will be assumed for ρ_T.

	$L_o(1)$ dBc/Hz	B_L Hz	σ_o^2 rad^2
USO	-45	0.5	0.002
SDST Aux Osc	-20	2	0.044
Cassini Aux Osc	-13	5	0.035

Table 3: Oscillator Parameters

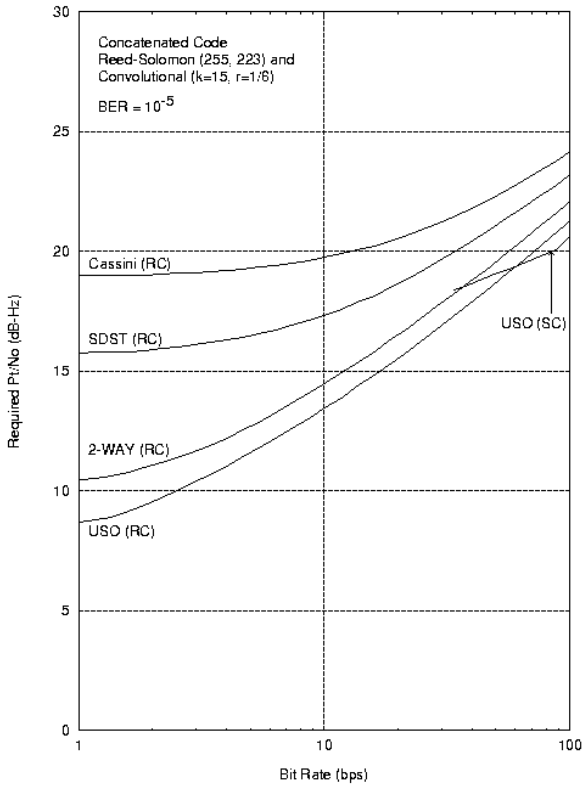

Figure 3: Minimum Required P_T/N_0 as a Function of Bit Rate

Figure 3 plots the minimum required P_T/N_0 that just satisfies the two constraints that are summarized by inequalities (4) and (5). For each of the oscillators of Table 3, there is one curve representing telemetry performance for one-way, residual-carrier transmission with that oscillator as the source of the downlink carrier. In addition, there is a curve for two-way coherent, residual-carrier transmission with ρ_T = 15 dB. The label "RC" in the figure indicates residual carrier. There is also one curve for one-way, suppressed carrier ("SC") telemetry with a USO. The residual carrier curves were generated in such a way that at each point on a curve, the optimum modulation index is employed. In moving to the right along one of these curves (in the direction of larger R_b), the (optimum) modulation index is continuously increasing. For sufficiently large R_b, the four residual-carrier curves coalesce, meaning that telemetry performance becomes independent of the oscillator phase noise. However, for the low bit rates of interest in this report, telemetry performance is a strong function of the quality of the oscillator. Table 4 lists the minimum required P_T/N_0 for R_b = 5, 10 and 20 bps, and Table 5 lists the corresponding optimum modulation index. For the better oscillator, the USO, the optimum modulation index is larger than for the poorer oscillators. For the USO, a greater percentage of the signal power can be devoted to the modulation sidebands and less to the residual carrier because it has been possible to use a smaller B_L in the receiver.

Bit Rate	*5 bps*	*10 bps*	*20 bps*
USO	11.6	13.5	15.6
SDST Aux Osc	16.5	17.3	18.7
Cassini Aux Osc	19.3	19.8	20.5
Two-Way Coherent	12.7	14.5	16.5

Table 4: Minimum Required P_T/N_0, dB-Hz

Bit Rate	*5 bps*	*10 bps*	*20 bps*
USO	50°	55°	60°
SDST Aux Osc	27°	36°	46°
Cassini Aux Osc	18°	26°	35°
Two-Way Coherent	46°	54°	59°

Table 5: Optimum Modulation Index

Table 6 shows the system loss η_{SL} corresponding to the operating conditions shown in Tables 4 and 5.

Bit Rate	*5 bps*	*10 bps*	*20 bps*
USO	-2.0	-1.4	-1.0
SDST Aux Osc	-2.3	-2.4	-2.5
Cassini Aux Osc	-2.0	-2.2	-2.3
Two-Way Coherent	-2.6	-2.3	-1.8

Table 6: System Loss

With residual-carrier telemetry, as R_b decreases the optimum modulation index decreases, meaning a greater percentage of the signal power is diverted to the residual carrier. This might suggest that low bit rate telemetry is an ideal candidate for suppressed-carrier transmission. Ironically, just the reverse is true. At low bit rates the constraint expressed by inequality (5), which concerns the quality of phase-lock in the carrier synchronization circuit, becomes the dominant consideration. In other words, for low bit rates it is easy to satisfy inequality (4), so telemetry performance is dictated by what goes on in the phase-locked loop. Unlike Costas loops, residual-carrier phase-locked loops cannot slip half-cycles and so can be operated with a considerably larger σ_ϕ^2. Figure 3 shows a curve for one-way, suppressed-carrier transmission with a USO. For one-way transmission with a USO, residual carrier offers better performance than suppressed carrier for R_b < 60 bps. For the other oscillators, the bit rate below which residual carrier is better occurs at bit rates that are off the right side of Figure 3.

The minimum required PFD is found from equation (3) and Tables 2 and 4. The results are given in Table 7. Each entry in this table consists of two numbers (both in units of dBW/m^2): the first for a 70 m antenna with a HEMT LNA and the second for a 34 m beam-waveguide antenna. Diplexed operation is assumed for two-way coherent; non-diplexed operation is assumed otherwise.

Bit Rate	*5 bps*	*10 bps*	*20 bps*
USO	-236.3/ -230.0	-234.4/ -228.1	-232.3/ -226.0
SDST Aux Osc	-231.4/ -225.1	-230.7/ -224.3	-229.2/ -222.9
Cassini Aux Osc	-228.6/ -222.3	-228.1/ -221.8	-227.4/ -221.1
Two-Way Coherent	-235.2/ -227.7	-233.4/ -225.9	-231.4/ -223.9

Table 7: Minimum Required Power Flux Density, dBW/m^2 (70 m HEMT/ 34 m BWG)

TEST RESULTS

The Near Earth Asteroid Rendezvous (NEAR) spacecraft, launched February 17, 1996, has an emergency telemetry mode at 9.9 bps with a 53° modulation index. Extensive testing with the Block V receiver validated link performance in this mode using a 1 Hz tracking loop bandwidth. Because the NEAR spacecraft has a Cassini transponder and no USO, it requires a coherent downlink in this mode. BER testing indicated a system loss of -2 dB at 9.9 bps (compare to -2.3 dB predicted in Table 6).

The NEAR telecom team noted that ground system acquisition performance is also critically important at low data rates. This is an often overlooked part of the de-

sign. Many functional elements of the system must achieve synchronization, including the carrier loop, subcarrier loop, symbol synchronizer, convolutional decoder, frame synchronizer, and Reed-Solomon decoder. Experience with NEAR has shown that the acquisition of all three Block V loops (carrier, subcarrier, and symbol) occurs within 10 minutes at BER threshold conditions. However, if careful attention is not paid to the baseband configuration following the Block V, then significant delays can result. For example, the NEAR frame length is 8832 bits. If buffering within the convolutional decoder were set to its default of three frames, then acquisition would be delayed by 45 minutes (the buffering is set to one frame for NEAR). Future users should also be aware that the convolutional decoder will often false-lock at low symbol rates, requiring manual intervention that can delay acquisition by an additional hour.

The best way for future missions to reduce acquisition time is to reduce the CCSDS[6] frame length as much as possible. In addition, it is important to configure the DSN baseband equipment so that recovered data bits are sent to the end user immediately instead of buffering the data. This requires acceptance of a higher "false alarm" threshold for frame sync detection.

Conclusion

Designers of future deep space missions must be cognizant of the fundamental limitations of the DSN to receive very weak signals. They must ensure adequate oscillator stability, transmitter power and antenna gain to meet the minimum PFD limits denoted in Table 7. If they plan to use auxiliary oscillators in the weak signal regime, they must be able to adjust the modulation index to the levels shown in Table 5 to ensure optimal performance.

Somewhat higher performance than shown in Table 7 is possible by arraying multiple antennas. However, current plans commit to arraying only at the Goldstone complex, and even there arraying should be used only on an exceptional basis to minimize resource conflicts between missions.

Acknowledgments

The work described here was carried out at the Jet Propulsion Laboratory, California Institute of Technology under a contract with the National Aeronautics and Space Administration.

---

[1] Martin, Warren L., "DSN Support of Earth Orbiting and Deep Space Missions," March 1994, available on the World Wide Web at http://deepspace1.jpl.nasa.gov/advmiss/.

[2] J. B. Berner and K. M. Ware, "An Extremely Sensitive Digital Receiver for Deep Space Satellite Communications," *Eleventh Annual International Phoenix Conference on Computers and Communications*, pp. 577-584, Scottsdale, Arizona, April 1-3, 1992.

[3] J. H. Yuen, editor, *Deep Space Telecommunications Systems Engineering*, Plenum Press, New York, 1983.

[4] L. C. Palmer and S. A. Klein, "Phase Slipping in Phase-Locked Loop Configurations That Track Biphase or Quadriphase Modulated Carriers," *IEEE Transactions on Communications*, pp. 984-991, October 1972.

[5] D. Halford, J. H. Shoaf, and A. S. Risley, "Spectral Density Analysis: Frequency

Domain Specification and Measurement of Signal Stability," *Proceedings of the 27th Annual Symposium on Frequency Control 1973*, Cherry Hill, New Jersey, 1973, pp. 421-431. (Also published as *NBS Technical Note 632*.)

[6] Consultative Committee for Space Data Systems. *See* CCSDS Documents Library on the World Wide Web at http://joy.gsfc.nasa.gov/CCSDS-DocLib.html.